

Nanocerium oxide increases the survival of adult rod and cone photoreceptor in culture by abrogating hydrogen peroxide-induced oxidative stress

Neelima Bhargava, Vellasamy Shanmugaiah, Manav Saxena, Manish Sharma, Niroj Kumar Sethy, Sushil Kumar Singh, Karuppiah Balakrishnan, Kalpana Bhargava, and Mainak Das

Citation: *Biointerphases* **11**, 031016 (2016); doi: 10.1116/1.4962263

View online: <http://dx.doi.org/10.1116/1.4962263>

View Table of Contents: <http://scitation.aip.org/content/avs/journal/bip/11/3?ver=pdfcov>

Published by the AVS: Science & Technology of Materials, Interfaces, and Processing

Articles you may be interested in

[Toxicological evaluation of dextran stabilized iron oxide nanoparticles in human peripheral blood lymphocytes](#)
Biointerphases **11**, 04B302 (2016); 10.1116/1.4962268

[Antimicrobial activity of tantalum oxide coatings decorated with Ag nanoparticles](#)
J. Vac. Sci. Technol. A **34**, 04C102 (2016); 10.1116/1.4947077

[Nanoceria based electrochemical sensor for hydrogen peroxide detection](#)
Biointerphases **9**, 031011 (2014); 10.1116/1.4890473

[Size-dependent ferrohydrodynamic relaxometry of magnetic particle imaging tracers in different environments](#)
Med. Phys. **40**, 071904 (2013); 10.1118/1.4810962

[Nanostructured magnesium oxide biosensing platform for cholera detection](#)
Appl. Phys. Lett. **102**, 144106 (2013); 10.1063/1.4800933

Nanocerium oxide increases the survival of adult rod and cone photoreceptor in culture by abrogating hydrogen peroxide-induced oxidative stress

Neelima Bhargava

Department of Microbial Technology, School of Biological Sciences, Madurai Kamaraj University Madurai, Tamil Nadu 625021, India and Biological Sciences and Bioengineering, Indian Institute of Technology Kanpur, Kanpur, Uttar Pradesh 208016, India

Vellasamy Shanmugaiyah^{a)}

Department of Microbial Technology, School of Biological Sciences, Madurai Kamaraj University Madurai, Tamil Nadu 625021, India

Manav Saxena

Biological Sciences and Bioengineering, Indian Institute of Technology Kanpur, Kanpur, Uttar Pradesh 208016, India

Manish Sharma and Niroj Kumar Sethy

Defense Institute of Physiology and Allied Sciences, Defense Research Development Organization, Lucknow Road, Delhi 110056, India

Sushil Kumar Singh

Solid State Physics Laboratory, Defense Research Development Organization, Lucknow Road, Delhi 110056, India

Karuppiyah Balakrishnan

Department of Immunology, School of Biological Sciences, Madurai Kamaraj University, Madurai, Tamil Nadu 625021, India

Kalpana Bhargava

Defense Institute of Physiology and Allied Sciences, Defense Research Development Organization, Lucknow Road, Delhi 110056, India

Mainak Das^{a)}

Biological Sciences and Bioengineering, Indian Institute of Technology Kanpur, Kanpur, Uttar Pradesh 208016, India and Design Program, Indian Institute of Technology Kanpur, Kanpur, Uttar Pradesh 208016, India

(Received 4 April 2016; accepted 24 August 2016; published 16 September 2016)

In vitro cell culture system for adult rod and cone photoreceptor (PR) is an effective and economical model for screening drug candidates against all kinds of age related retinal blindness. Interestingly, adult PR cells have a limited survival in the culture system, thus preventing full exploitation of this *in vitro* approach for drug screening applications. The limited survival of the adult PR cells in culture is due to their inherently high oxidative stress and photic injury. Mixed valence-state ceria nanoparticles have the ability to scavenge free radicals and reduce oxidative stress. Here, ceria nanoparticles of 5–10 nm dimensions have been synthesized, possessing dual oxidation state (+3 and +4) as evident from x-ray photoelectron spectroscopy and exhibiting real time reduction of hydrogen peroxide (H₂O₂) as quantified by absorbance spectroscopy and cyclic voltammogram analysis. Using flow cytometry and cell culture assay, it has been shown that, upon one time addition of 10 nM of nanoceria in the PR culture of the 18 months old adult common carp (*Cyprinus carpio*) at the time of plating the cells, the oxidative stress caused due to hydrogen peroxide assault could be abrogated. A further single application of nanoceria significantly increases the survival of these fragile cells in the culture, thus paving way for developing a more robust photoreceptor culture model to study the aging photoreceptor cells in a defined condition. © 2016 American Vacuum Society. [<http://dx.doi.org/10.1116/1.4962263>]

I. INTRODUCTION

Millions of people over the age of 65 years suffer from age related retinal blindness like inherited retinal degeneration,

macular degeneration, diabetic retinopathy, and retinal detachment.^{1–6} An *in vitro* cell culture model of adult photoreceptor (PR) cells could be an effective and economical tool, to understand the molecular progression of these age related disorders in a controlled environment, and to screen putative drug candidates against these disorders. Currently, very few long term adult photoreceptor cell culture models are

^{a)}Authors to whom correspondence should be addressed; electronic mail: mainakd@iitk.ac.in

available.^{7–13} Interestingly, in all the existing culture models, there is limited survival of the adult PR cells. The major reasons for such limited survival of PR cells in culture are the following: First, due to the inherent high oxygen metabolism of the PR cells, they are continuously exposed to oxidative stress which is elucidated by the generation of large quantity of free radicals. Second, light exposure leads to photic injury due to the photo-chemical reaction with the chromophores present in the PR cells. Irrespective of the initial cause of damage, the key reason for the PR cell death is the excessive burden of free radicals leading to oxidative stress.^{14–25}

Thus, the critical question is “how to minimize the burden of free radicals in an *adult PR culture*?.” Certain clues could be obtained from few earlier findings, where *adult central nervous system neurons* have been cultured successfully in a defined system.^{26–29} Studies attempted to culture *adult rat or mouse spinal cord motoneuron and hippocampal neurons* documented that “autocatalytic cerium oxide nanoparticles offer neuroprotection to adult rat and mouse spinal cord and hippocampal neurons.”^{26–29} These studies demonstrated that single dose application of nanoceria at a nanomolar concentration at the time of plating the adult neuronal cells is biocompatible, regenerative, and provides significant neuroprotection and longer survival of the neurons in the culture.^{26–29} The next obvious question is “how ceria acts in an aqueous system and offers neuroprotection?”

Cerium oxide nanoparticles offer neuroprotection by exhibiting antioxidative properties. It acts in two putative ways: (1) as an *antioxidant enzyme mimetic* like catalase mimetic (scavenging hydrogen peroxide) or as a superoxide-dismutase (SOD) mimetic scavenging super-oxide species; (2) exhibiting reactive oxygen species (ROS)/reactive nitrogen species scavenging activity.^{26–44} The next question is how ceria exhibit antioxidative activity in aqueous solution. A part of the answer lies in the surface chemical features of nanoceria and the subsequent interaction in an aqueous medium. The genesis of current understanding of “action of nanoceria” has evolved from the following three key discoveries made between 2006 and 2011. In 2006, Chen *et al.*³³ discovered that nanoceria particles offer neuroprotection to the neonatal rat retinal neurons in the primary culture, established from 0- to 2-day-old rat pups. Since the 0-to 2-day-old rat pup neurons have very high regeneration capacity, so it remained a question, whether this study could be translated to grow adult retinal PR neurons in the culture. This question remains unanswered prior to this study. Interestingly, the possibility that nanoceria could be used as a potential tool for the regeneration of the adult central nervous system (CNS) neurons in culture was demonstrated by Das *et al.* in 2007.^{26,27} It was shown that nanoceria help in regeneration of adult rat spinal cord neurons. This study indirectly suggested that ceria nanoparticles have the ability to remove hydroxyl radical formed from hydrogen peroxide in an aqueous medium, thus pointing toward innate peroxide scavenging potential of nanoceria.^{26,27} Four years later, in 2011, “the direct evidence for hydroxyl radical scavenging activity of cerium oxide nanoparticles” was provided by Xue *et al.*^{30,31}

Both these studies used x-ray photoelectron spectroscopy (XPS) to document that ceria in nanodimension exist in dual oxidation state (+3 and +4), and have the ability to swap between these two oxidation states in an autocatalytic manner. Thus, the key to free radical scavenging ability of ceria lies in its mixed valence-state. The present understanding is the following: Ceria nanoparticles have unique autocatalytic redox ability to scavenge free radicals and reduce oxidative stress. It mimics the activity of classical antioxidant enzymes like catalase and SOD.^{26–44}

As discussed in the earlier paragraphs that in terms of testing the possibility of enhancing the life span of adult PR cells in the culture (*ex vivo*) by treating them with nanoceria was not explored. Since the age related retinal blindness like inherited retinal degeneration, macular degeneration, diabetic retinopathy, and retinal detachment occurs due to the aging of PR neurons, so it is all the more imperative to target this unanswered question: “whether nanoceria could support the long-term survival of adult photoreceptor cells in the culture?” This question was logical and pertinent, since it was shown earlier that nanoceria support the survival of adult spinal cord neurons and neonatal PR neurons in the culture.^{26,27,33}

Thus, in this work, the efficacy of antioxidant ceria nanoparticles in ameliorating the oxidative stress caused to the adult PR cells in culture has been tested. This necessitates the following: (1) synthesis of the ceria nanoparticles; (2) microscopic, spectroscopic,^{40,41} and electrochemical^{40,45} characterization of the ceria nanoparticles; (3) evaluating the survival of the adult PR cells in culture when challenged with hydrogen peroxide (H₂O₂), both in the presence and absence of nanoceria; (4) evaluating the survival of adult PR cells in culture upon priming with ceria nanoparticles at the time of plating the cells.

II. EXPERIMENT

A. Synthesis, reaction mechanism, temperature consideration, and yield of cerium oxide nanoparticles

Nano ceria were synthesized by reacting 0.025 M aqueous solution of Ce(NO₃)₃·6H₂O (Aldrich, USA; CAS No. 10294-41-4) with 0.025 M aqueous solution of hexamethylenetetraamine (HMTA, Sigma-Aldrich, USA; CAS No. 100-97-0) at a temperature of 75 °C for 4 h. The reaction vessel was continuously stirred. HMTA acts a capping agent. The resultant white turbid solution was centrifuged at 12 000 rpm for 2 min and washed with milli-Q water and acetone thrice and stored in vacuum desiccator for drying and further used for the experiments.⁴⁰ The water used for making solutions was obtained from milli-Q[®] integral water purification system (Milli-Q-EMD Millipore system).

The synthesis of ceria nanoparticles can be explained by the following mechanistic pathway. HMTA decomposes to formaldehyde and ammonia in aqueous medium upon heating, thus increasing the hydroxyl ion concentration in the solution. This hydroxyl ions react with Ce³⁺ ions of Ce(NO₃)₂·6H₂O to form Ce(OH)₃. Since Ce(OH)₃ is

unstable in an aqueous solution and it readily undergoes an aerial oxidation process to produce $\text{Ce}(\text{OH})_4$ in the form of a precipitate. This $\text{Ce}(\text{OH})_4$ is further hydrolyzed to CeO_2 by losing the hydroxyl groups. The reaction is as follows:



The temperature is a critical consideration in obtaining well dispersed ceria nanoparticles. It is well known that the decomposition of HMTA is very slow in room temperature. So, it is very difficult to produce sufficient amount of ammonium hydroxide in an aqueous medium at room temperature. Thus, by increasing the temperature of the solution, hydrolysis of HMTA could be hastened. But the increase in temperature has to be controlled and fixed at around 75°C . At a temperature higher than 80°C , large amount of hydroxyl ions are produced at a rapid pace, resulting in a very basic environment, which causes agglomeration of the product. So, HMTA assisted growth procedure of ceria nanoparticles can be moved in the forward direction by adjusting the reaction temperature at 75°C .

Based on the above reaction, the theoretical and actual yield could be calculated. It can be assumed that 1000 ml of 1 M $\text{Ce}(\text{NO}_3)_2 \cdot 6\text{H}_2\text{O}$ (MW 434.22 g) can produce 1 M Ce^{3+} , which upon subsequent oxidation, followed by hydrolysis, produces 1000 ml 1M CeO_2 , i.e., 172.12 g, as the MW of cerium oxide is 172.12 g. So accordingly, 1000 ml of 1 M $\text{Ce}(\text{NO}_3)_2 \cdot 6\text{H}_2\text{O}$ upon hydrolysis by HMTA produces 172.12 g CeO_2 . Thus, 100 ml of 0.025 M solution of $\text{Ce}(\text{NO}_3)_2 \cdot 6\text{H}_2\text{O}$ produces $172.12 \times 0.025/10 = 0.403$ g of CeO_2 . This is the theoretical yield. The experimental yield of ceria nanoparticles using $\text{Ce}(\text{NO}_3)_2 \cdot 6\text{H}_2\text{O}$ upon hydrolysis by HMTA results in 0.290 g* of product. The asterisk (*) indicates the actual yield of pure product. Certain amount of loss is incurred during washing and centrifugation, which is unavoidable. So, the actual yield % is given by the following equation: [(Experimental yield/Theoretical Yield) \times 100%]. Accordingly, the percentage yield for this above described method of synthesis is $\sim 71\%$ [(0.290/0.403) \times 100%].

B. Characterization of the cerium oxide nanoparticles

The shape of the particles was characterized using high resolution transmission electron microscopy (HRTEM) using JEOL transmission JEM2000FX system, having a STM equipped with a Quantum detector. The crystal structure and the particle size of the synthesized nanocerium were determined by powder x-ray diffraction (XRD) using a PANalytical XRD system. The surface chemical features of the synthesized particles were explored using XPS analysis using PHI 5000 Versa Probe II, FEI, Inc.

C. Studying the quenching of hydrogen peroxide by ceria nanoparticles using absorption spectroscopy

An instant reaction between H_2O_2 and V_2O_5 (vanadium pentoxide), in the presence of H_2SO_4 (sulfuric acid), resulted in the formation of a peroxovanadate complex, which has an absorption maxima at 454 nm. Thus, by quantifying the

absorbance, the peroxide level could be quantified. This novel technique of H_2O_2 estimation was developed earlier by Zhang *et al.* to determine peroxide in bleaching effluents.⁴⁵ This technique has been adopted here to study the peroxide quenching ability of ceria. In the control experiment, pure H_2O_2 (Fisher Scientific, Mumbai, India; 18755/066141013) was reacted with 0.2 g V_2O_5 (S.D. fine Chem., Ltd., Mumbai, India; L99a/0884/0899/31) in 100 ml 0.5 M H_2SO_4 (Sigma-Aldrich, USA; CAS No.: 7664-93-9), and the absorbance spectrum was recorded at 454 nm. In the test sample, 100 mg nanocerium was incubated along with same quantity of H_2O_2 , and to this mixture, 0.2 g V_2O_5 in 100 ml 0.5 M H_2SO_4 was added. The absorbance spectra of control and the test sample were compared.

D. CV analysis to verify the reduction of hydrogen peroxide by nanocerium

Cyclic voltammogram (CV) analysis was performed to study the peroxide quenching ability of nanocerium by reducing peroxide molecules. The working electrode was prepared with cerium by spraying 30 mg of nano- CeO_2 (prepared by mixing and sonicating in 3 ml isopropyl alcohol and 30 μl of $6\times$ diluted nafion [solution for 3 h, where nafion (Sigma-Aldrich, USA; MKBP9895V/70160-25m) functions as a binder] on one side of the indium tin oxide (ITO) sheet. ITO sheets were obtained from Techinstro, Nagpur, India (TIX005). Phosphate buffer saline (PBS) was freshly prepared and used as the electrolyte, and the pH was adjusted at 7.4. Epsilon Basi C3 cell stand with a conventional three electrode configuration was used for recording the CV, where Ag/AgCl was used as the reference electrode and platinum as the counter electrode. CV was performed at different scan rates from 10 to 300 mV/s between a voltage window of -0.8 to 0.8 V.

E. Rod and cone PR cell culture from the common carp (*Cyprinus carpio*) and H_2O_2 treatment

The PR cells were isolated from adult carp. The detailed protocol for isolation and culture has been documented in an earlier work by Bhargava *et al.*¹² The overall procedure from dissection to cell plating is shown schematically in Fig. 1. Adult carp fishes are maintained in the laboratory aquarium under optimal conditions as described earlier.¹² Approximately 18 000 live PR cells could be harvested from one pair of adult carp retina, as reported earlier by Bhargava *et al.*¹² At the time of plating, 3000 PR cells were seeded on each coverslip, having a dimension of 22×22 mm². Since these cells have an elongated morphology, a low density culture (~ 6 cells/mm²) was followed, so that cells get optimal space to spread out and grow. The cells were plated on concanavalin A substrate. The concanavalin A plates were prepared 6 h prior to start of the culture. Cells were dissected from the adult carp retina and maintained in L15 medium (500 ml) supplemented with B27 (10 ml), glutamax (5 ml), and antibiotic and antimycotic (5 ml) in ambient environment without any additional requirement of carbon dioxide incubator. The relative humidity was maintained at 80%.¹²

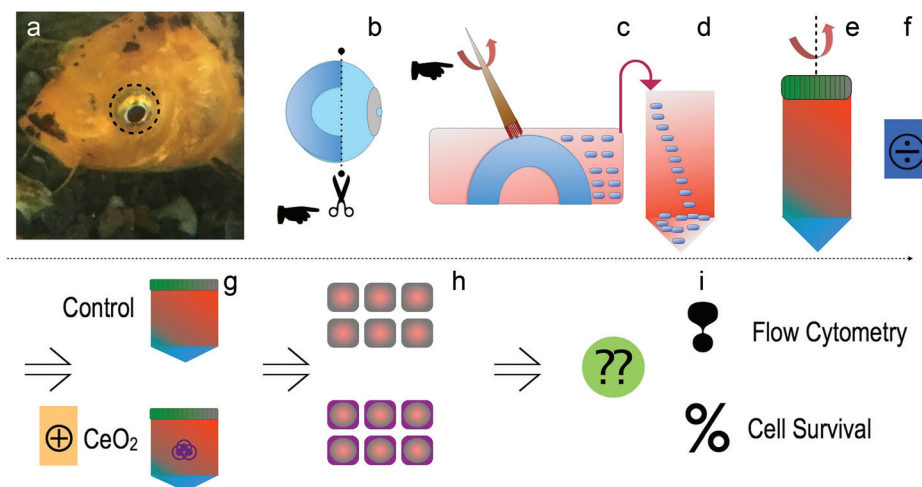


FIG. 1. Overall schematic of the dissection to cell plating process: (a) An 18 month old adult carp maintained in the aquarium. (b) Dissecting the whole eye, cutting open the eye ball to remove the whole retina from back of the eye. It is a critical step and need to be performed very carefully. Retina is shown in dark blue semicircle on the back side of the eye ball; (c) Isolated retina is placed in the dissecting medium, kept on the dish. Using a fine brush, the PR cells were detached from the retina. This step is exceptionally delicate and needs to be performed very gently, since the PR cells are loosely adhered to the retina. The PR cells are shown as small rounded blue rectangles. (d) The isolated cells along with the medium is aspirated out in a sterilized test tube. (e) The cell suspension is spin down at 300 g for 5 min. (f) The pelleted cells are resuspended in fresh medium and divided into two equal parts: (g) One part is used as control and in the other part CeO_2 is added. (h) Equal number of cells from each group is plated on concanavalin A coated coverslips; (i) The key assays performed in this study are flow cytometry assay and the percentage PR cell survival in control and CeO_2 treated cultures.

The cultures were divided into two groups, viz., control and ceria treated (10 nM). Nanoceria treatment was given only once, at the time of plating the cells. Hydrogen peroxide (H_2O_2) treatment was done one day after the culture has stabilized. An earlier study by Bhargava *et al.* on adult PR cells showed that cells adhere and stabilized during first 24 h after plating.¹² Thus, all the assays are performed once the plated population stabilized in the culture. A 30 μM of H_2O_2 treatment was given and left for 1 h. After 1 h, the flow cytometry assay was performed to evaluate the live and dead cells. There were four different groups which were assayed, viz., control, control + H_2O_2 , ceria, and ceria + H_2O_2 . The above mentioned chemicals were obtained from the following sources: Leibovitz's L15, Himedia laboratories, India, Catalog No. AT011; B27 Supplement, Gibco[®], Life technologies[™], Catalog No. 17504-044; GlutaMAX[™] Supplement, Gibco[®], Life technologies[™], Catalog No. 35050-061; 100 \times Antibiotic-antimycotic, Gibco[®], Life technologies[™], Catalog No. 15240-062; Life technologies, live/dead viability/cytotoxicity assay kit (L-3224) was used for quantifying the viability the adult PR cells in the culture.

F. Flow cytometry

Flow cytometry was performed using FA Scalibur (Becton Dickinson) instrument. ROS dependent cell death induced by H_2O_2 in the PR cells was measured using propidium iodide (PI) fluorescent probe. PI permeates inside the dead cells through damaged cell membrane and therefore stains the dead cells (PI⁺), while the live cells are not stained (PI⁻) since the cell membrane integrity is maintained. The assay was initiated by trypsinizing (0.25% trypsin-EDTA solution) the PR cells and pelleting them after centrifuging at 1500 rpm for 10 min. The trypsin was obtained from Sigma-Aldrich, USA (T4299).

Following this, cells were washed three times with PBS and incubated with 10 μM of PI solution and 25 μM of 2',7'-carboxy-methyl-dichloro-dihydro-fluorescein diacetate (CM-DCF₂DA, cat# C6827, Life Technologies) solution at 37 °C for 15 min. CM-DCF₂DA is a fluorescent probe which binds to the ROS. The cells were washed, resuspended in 500 μl PBS, and transferred to fluorescence-activated cell sorting tubes. The fluorescence intensity of CM-DCF₂DA was monitored at the FL-1 channel and 10 000 events were collected per sample; whereas in FL-2 channel the fluorescence intensity of PI⁺ cells were recorded (10 000 events were collected per sample).

G. Rod and cone photoreceptor culture assay

Cell culture assay was performed for control and control + ceria (10 nM) treatment. Ceria treatment was given only once at the time of plating the cells. Equal number of cells was plated in both the cultures. (Cell plating density is described in earlier paragraph.) The data were sampled from five independent cultures. The cells were maintained for 6 days, and the viable cells were quantified at day 6, using live dead assay kit (Cat # L3224, ThermoFisher Scientific). The methodology for using the assay kit is provided by the manufacturer. The live PR cells showed green fluorescence, when incubated with the dye for 15 min. The green fluorescent labeled live PR cells are counted for analysis. The cells were visualized using fluorescent Zeiss inverted microscope.

III. RESULTS

A. Nanoceria synthesis

Nanoceria were synthesized by a low temperature (75 °C), low energy intensive route using HMTA as a

capping agent. The reaction mechanism, significant of the temperature consideration and the theoretical/experimental yield, has already been discussed in Sec. II. Here, it is noteworthy that, in one of the earlier work by Ujjain *et al.*, nanoceria were synthesized by the above route, to develop an ultrasensitive electrochemical sensor for detecting trace amount of hydrogen peroxide.⁴⁰

B. HRTEM, XRD, and XPS analyses

HRTEM image showed that the average particle size varies between 5 and 10 nm and have rhomboidal morphology with rounded corners and smooth texture. Such rounded corners and smooth texture are desirable features since these minimize any form of physical or mechanical damage to the cells [Fig. 2(a)]. Earlier few researchers have observed cellular toxicity with ceria particles, which were either procured from commercial vendors or synthesized at higher temperature, thus resulting in particles having sharp edges because of high temperature synthesis. On the contrary, a low temperature synthesis could result in harnessing the benefits of these particles.

In the HRTEM method, nanoparticles may aggregate, and it is hard to distinguish the nanoparticles boundaries to calculate the exact particles size. So, one of the approach would be to use powder x-ray diffraction (PXRD), which is one of the accurate technique to analyze the crystallite size. The Scherrer equation ($Dp = 0.94\lambda/\beta_{1/2} \cos\theta$) was used to calculate the crystallite size, where Dp is the average crystallite size, β is the spectral line broadening [full width at half maximum (FWHM)], θ is the Bragg angle, and λ is the x-ray wavelength. The crystallite size of the synthesized CeO₂ is

8.32 nm calculated using the Scherrer equation from the XRD peak positioned at $2\theta = 28.53^\circ$ with FWHM 1.03° [refer to Fig. 2(b)]. CeO₂ particles showed distinct and sharp diffraction peaks corresponding to (111), (200), (220), and (311) lattice planes of CeO₂ cubic phase. This is in agreement with the previously reported XRD data [Fig. 2(c)].⁴⁰

The composition and chemical state of Ce were analyzed by XPS technique. The broad XPS peak could be deconvolute into peaks related to the spin-orbit coupling. The peaks v_0 , v , v' , v'' , and v''' are attributed to the Ce3d_{5/2} while u , u' , u'' , and u''' are assigned to the Ce3d_{3/2} ionization. The peaks v , v'' , v''' , u , u'' , and u''' belong to Ce⁺⁴ oxidation state while v_0 , v' , and u' are assigned to Ce⁺³ oxidation state of Ce.^{26-28,30,37,40} The XPS analysis shows that Ce⁺⁴ and Ce⁺³ coexisted on the surface [Fig. 2(d)]. In the Ce3d XPS of CeO₂ nanoparticles, due to the spin-orbit coupling, ten peaks have been analyzed, as per the convention. The standard notations of these bands are v_0 , v , v' , etc. So, due to the standard notation of bands originating from spin-orbit coupling, the above notations have been used.³⁷ Interestingly, a rising background was observed in the XPS spectra. The reason for the rising background is the following: In the XPS analysis, the electrons from deeper below the surface lose energy and emerge with reduced kinetic energy (increased apparent binding energy). Electrons very deep in surface lose all energy and cannot escape. The background is formed by the electrons that undergo inelastic loss processes before emerging. XPS spectra show characteristic “stepped” background (the intensity of the background toward higher binding energy is always greater than that toward lower binding energy) as observed in the present case, as earlier documented in the literature.^{46,47}

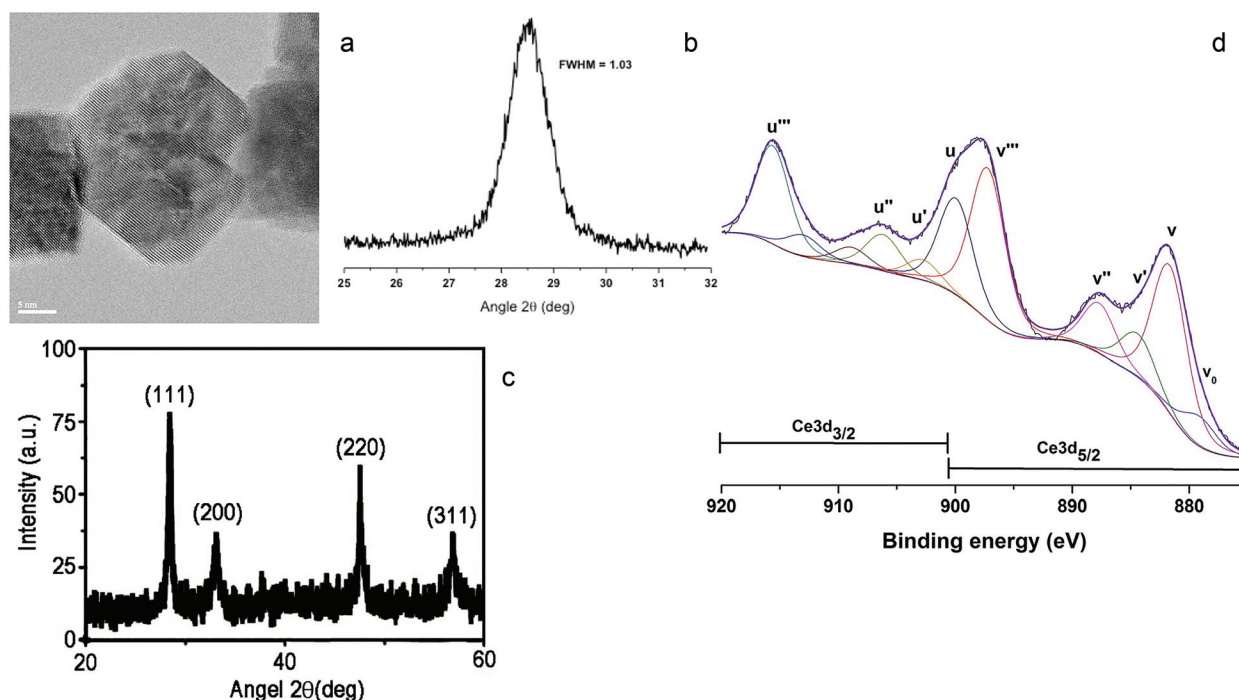


FIG. 2. Characterization of ceria nanoparticles. (a) HRTEM image. (b) PXRD for calculating particle size. (c) XRD analysis. (d) XPS.

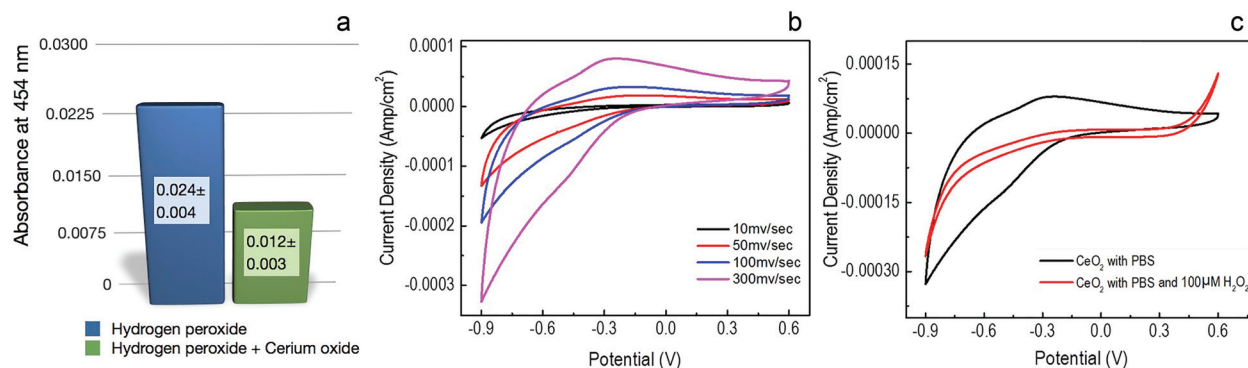


FIG. 3. Nanoceria quenching hydrogen peroxide. (a) Characteristic absorbance of the peroxovanadate complex at 454 nm is shown for $\text{H}_2\text{O}_2 + \text{V}_2\text{O}_5$ (blue bar) and $\text{H}_2\text{O}_2 + \text{V}_2\text{O}_5 + \text{CeO}_2$ (green bar). The data are shown as “mean absorbance \pm standard deviation” obtained from six independent experiments. (b) CV of nanoceria electrode in phosphate buffer saline at voltage range between -0.9 and 0.6 V, while following a scan rate of 10 – 300 mv/s. (c) Comparing the magnitude of current at the CeO_2 electrode, before and after addition of H_2O_2 ($100 \mu\text{M}$). Addition of peroxide significantly increases the peak current, thus indicating the electrocatalytic activity of CeO_2 .

C. Visualizing hydrogen peroxide quenching by nanoceria using absorbance spectroscopy

In the control experiments, pure H_2O_2 was allowed to react with V_2O_5 , thus resulting in the formation of peroxovanadate complex. This complex exhibited a characteristic absorbance at 454 nm [Fig. 3(a), blue color bar]. On the other hand, in the test sample, along with “ $\text{H}_2\text{O}_2 + \text{V}_2\text{O}_5$,” nano- CeO_2 was added. A significant reduction in the absorbance was observed [Fig. 3(a), green color bar], thus signifying considerable reduction in the formation of the peroxo-vanadate complex. This result indicated the peroxide quenching ability of CeO_2 .

D. Real time quantification of hydrogen peroxide reduction by nanoceria using CV

The electrocatalytic ability of the ceria was further studied for the H_2O_2 redox reactions. In Fig. 3(b), the CV for the CeO_2 electrode is recorded under optimal conditions. In Fig. 3(c), the CV was recorded before and after injection of H_2O_2 . As observed here, the peak current magnitude for the redox couple at the CeO_2 electrode increased significantly, after the addition of peroxide. This clearly suggested that peroxide oxidation is facilitated by CeO_2 .³⁶

E. Rod and cone photoreceptor culture

Earlier, a simple adult PR culture assay was developed for rapid and economical screening of different pharmacological molecules.¹² The cells were isolated from the dissected retina of the adult fish (*C. carpio*). These cells exhibited the preference to grow on lectin (Concanavalin A) substrate. The cells were maintained in ambient environment. This culture does not require carbon dioxide incubator for buffering, thus making it a robust system to work.¹²

F. Flow cytometry assay

Since nano- CeO_2 efficiently reduces peroxide, the efficacy of CeO_2 in protecting the PR cells against H_2O_2 -induced cell

death was evaluated using flow cytometry. The assay was performed with five different adult PR cell samples obtained from five different adult carp retina. PI-based flow-cytometry assay was used as described in Sec. II. Four different groups were assayed, and the representative flow cytometry results are shown in Fig. 4(a). The four groups were: (a1) control; (a2) H_2O_2 treatment; (a3) ceria treatment; and (a4) ceria + H_2O_2 treatment. The comparison of the average percentage of PI^+ (dead) cells obtained from five different trials ($n = 5$) is shown as [mean % of PI^+ (dead) cells \pm standard deviation; $n = 5$]: (a1) control (33.6 ± 0.54); (a2) H_2O_2 treatment (36.4 ± 1.14); (a3) ceria treatment (27.0 ± 1.58); and (a4) ceria + H_2O_2 treatment (29.8 ± 0.83). With respect to the control (a1), there is a $\sim 6\%$ reduction in dead cells in ceria treated (a3) culture. Similarly, $\sim 7\%$ reduction in dead cells is observed in ceria + H_2O_2 treatment (a4) as against just H_2O_2 treatment (a2). The comparison of the mean fluorescence intensity (MFI) value (2',7'-dichlorofluorescein diacetate), indicating the population of free radical in the system, in a1–a4, is represented as (mean MFI \pm standard deviation; $n = 5$): (a1) control (86 ± 4.18); (a2) H_2O_2 treatment (200.2 ± 10.00); (a3) ceria treatment (49.4 ± 3.78); and (a4) ceria + H_2O_2 treatment (125.6 ± 3.84). It showed that in the presence of nano- CeO_2 , the MFI value significantly reduces, indicating the ROS or free radical scavenging power of CeO_2 . Thus, the ceria fortified cells showed lesser death and low free radical burden as compared to the nonceria fortified cells, as observed in the flow cytometry assay. These results are summarized in Figs. 4(a1)–4(a4). Figure 4(b1) showed the reduction of CM-DCFDH-DA positive cells following “ceria fortification + H_2O_2 assault” (green trace showing shift toward left), whereas the red trace showing the control and blue trace showing the H_2O_2 assault in the absence of ceria fortification. Figure 4(b2) showed that “ceria fortification” leads to lower ROS level in the culture, as compared to the control culture. This trend has already been observed in the MFI data. The characteristic reduction of CM-DCFDHDA positive cells, following ceria fortification + H_2O_2 assault, was observed in all the five trials,

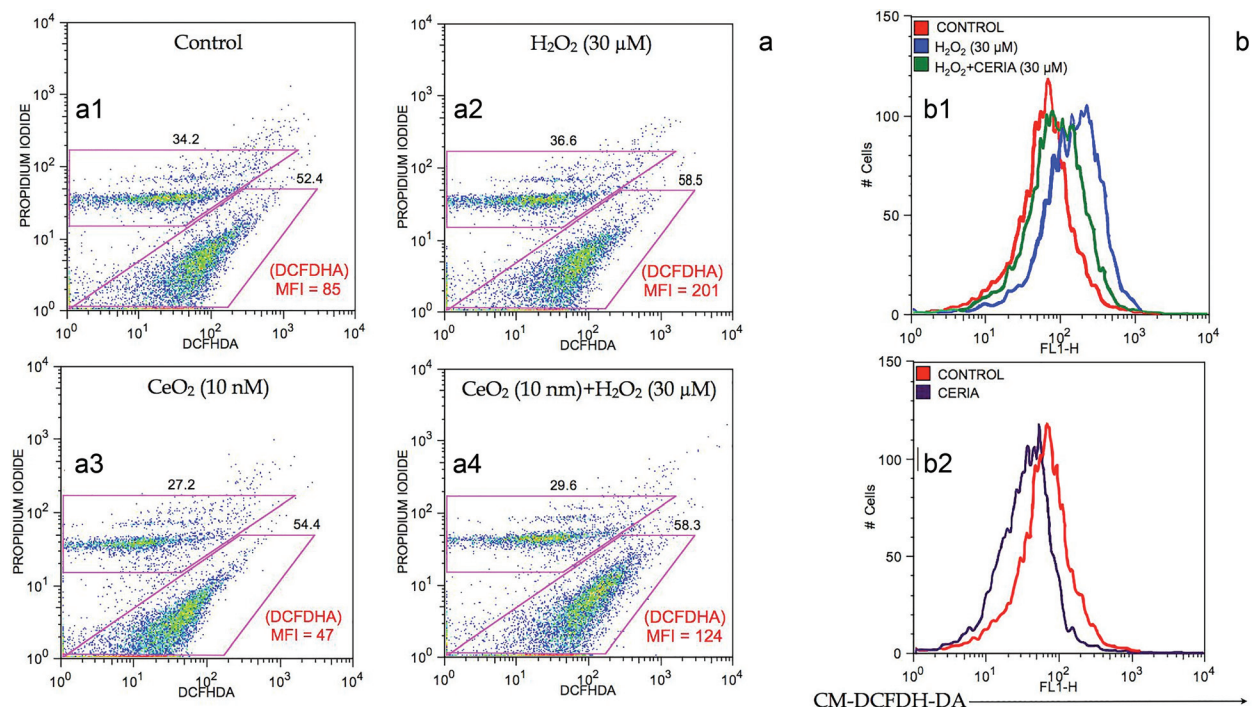


FIG. 4. Flow cytometry assay of rod and cone photoreceptor cells. (a) Comparing the PI⁺ cells in: (a1) control, (a2) H₂O₂ treated, (a3) ceria fortified, and (a4) ceria fortification + H₂O₂ treated. (b) Proportion of CM-DCFHDH-DA positive cells in (b1) control, ceria, and ceria + H₂O₂ treated. (b2) Comparing the CM-DCFHDH-DA positive cells in control vs ceria. The shift in the left showed reduction in ROS. The ceria fortification resulted in reduction in ROS in culture.

and a left shift is observed in all the cases. The next question was “does peroxide scavenging ability of ceria offers longer survival of the adult PR cells in the culture?” In Sec. III G, the cell culture studies have been discussed.

G. Photoreceptor survival in culture

Two population of cultures were maintained, viz., control and ceria treated. At day 6, the cultures were evaluated for the survival of the rod and cone cells. The ceria treatment at the time of plating the cells resulted in significantly higher survival of both rod and cone cells in the culture day 6. Ceria fortification at the time of plating the cells is possibly reducing ROS damage caused to the cells (Fig. 5).

IV. DISCUSSION

The results of the current study have been discussed under the following framework of observations:

- (1) translating the *ex vivo* application of nanocerium from neonatal PR cells³³ to adult PR cells;
- (2) the consilience of the role of ceria in two classes of vertebrates, viz., mammals and fish;
- (3) emerging evidences of significant role of nanocerium in the adult central nervous system culture;
- (4) ceria supplementation in cell culture medium for adult CNS culture and for organ preservation and transport;
- (5) ceria fortification for survival in extreme environment.

The overall summary of the discussion has been shown graphically in Fig. 6.

A. Translating the *ex vivo* application of nanocerium from neonatal PR cells to adult PR cells

The premise of this study is to test “whether nanocerium could support the long-term survival of adult photoreceptor cells in the culture, since earlier it has been shown that it supports survival of neonatal PR cells³³ in culture.” The present findings showed that *ex vivo* adult PR survival is significantly enhanced upon fortification with nanocerium. Here, it is worth mentioning that the adult PR cell culture is by far one of the most challenging adult CNS culture due to the extreme vulnerability of the adult PR cells to severe oxidative stress, photic injury, and physical injury during cell isolation process. Further the present findings support the emerging concept that nanocerium could be a potential therapeutic molecule to fight against the age related retinal blindness since it offers neuroprotection to the adult PR cells.

B. Consilience of the role of ceria in two different classes of vertebrates, viz., mammals and fish

The earlier studies which were performed on understanding the antioxidant role of ceria were carried out in mammalian systems.^{26–44} In the present study, similar antioxidant activity was observed in adult fish PR neurons. This offers a new experimental animal tool to explore the long-term genetic effects of nanoparticle treatment. If future, this study

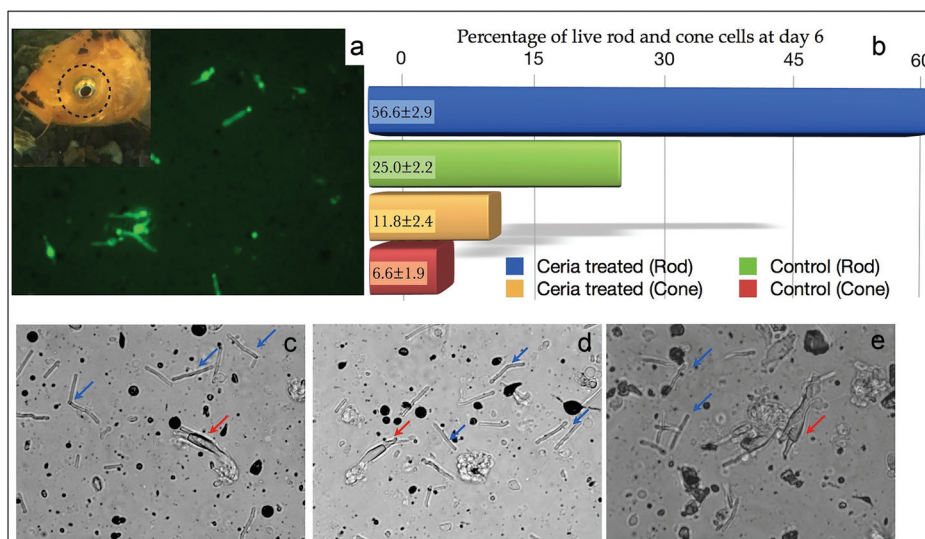


FIG. 5. Photoreceptor culture. (a) Representative picture of an 18 month old carp, which were used for isolating the rod and cone cells for the culture. A representative picture of the 6 days old live PR cells in culture are shown. The live cells (green) are fluorescent labeled. (b) At day 6, the percentage of live rod and cone cells were quantified in control and ceria treated cultures, and the results are shown in the form of bar graph (mean % of live cells ± standard deviation; n = 5). (c)–(e) Representative pictures of rod and cone cells in the culture at day 6. The rods are shown with blue arrows, and the cones are shown with red arrows. The rods are more numerous as compared to the cones.

could be easily translated to zebra fish, whose genome is well characterized, thus offering an opportunity to study multiple generations, epigenetic influences, and dissecting multiple gene interactions.

C. Emerging evidences of significant role of ceria in the adult central nervous system culture

The present study was inspired from the fact that autocatalytic cerium oxide nanoparticles offer neuroprotection to

adult rat and mouse spinal cord and hippocampal neurons.^{26–29} This is the third kind of adult CNS neuron, viz., adult photoreceptor neurons, which upon ceria priming, survives longer in culture. These evidences are pointing toward the fact that ceria is a potential neuroprotective agent for the acute *in vitro* adult neuron culture models, which lacks the supporting cellular architecture equipped with antioxidant enzymes like superoxide dismutase (SOD), catalase, and glutathione peroxidase. Further more and more adult CNS

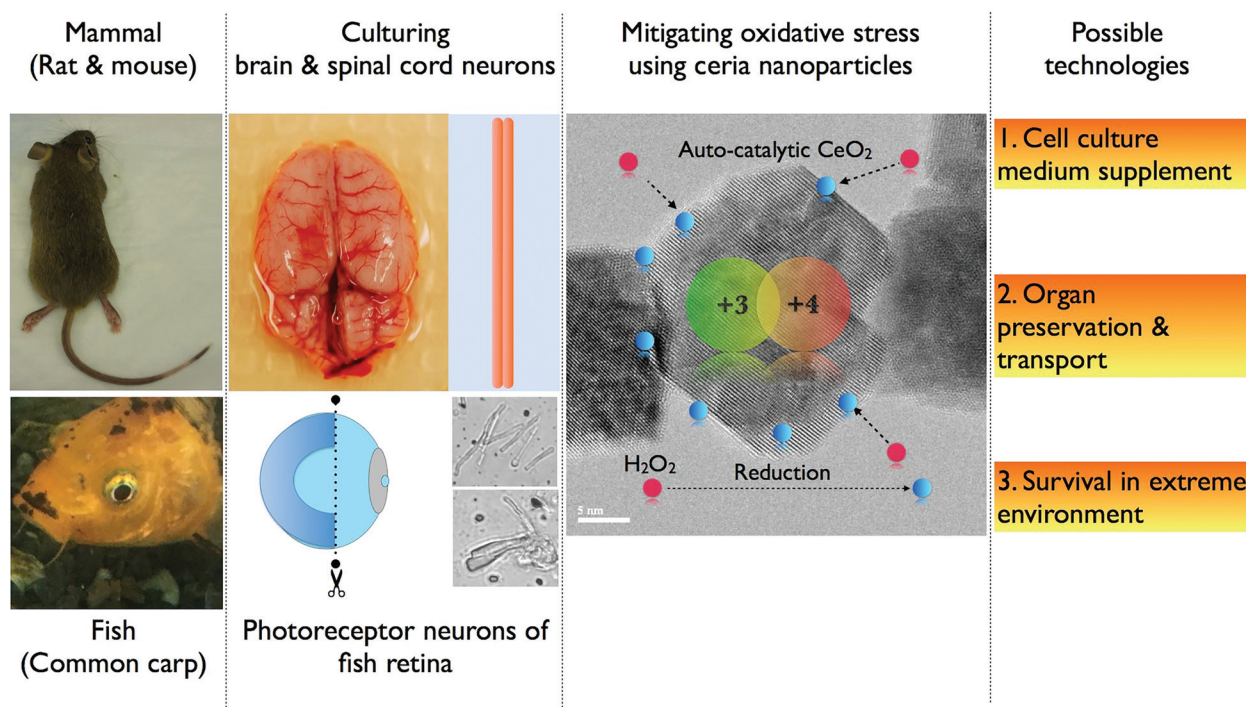


FIG. 6. Neuroprotective role of ceria in mammals and fishes. Enumerating the possible biomedical technologies using ceria nanoparticles.

culture models will be fruitful in addressing the age related neuronal maladies.

D. Ceria supplementation in cell culture medium for adult CNS culture and for organ preservation and transport

Following up the strings from the previous point, in future, ceria could be a potent “cell culture medium supplement,” for routinely growing adult CNS neurons. Thus, this approach of ceria fortification at the time of plating the cells offers the researchers a prolonged developmental window to explore the cellular and molecular aspects of the rod and the cone cells in the defined culture system. Further the antioxidative potential of ceria could be exploited in organ preservation and long distance transport where oxidative stress is a major challenge.⁴⁸

E. Ceria fortification for survival in extreme environments

Recent *in vivo* studies has shown that in the brain, it promotes neurogenesis and abrogate hypoxia-induced memory impairment and protect rodent lungs from hypobaric hypoxia-induced oxidative stress and inflammation.^{41,44}

V. CONCLUSION

Here, it has been shown that fortification of the adult photoreceptor culture with a single dose of nanoceria at the time of plating the cells significantly increases the survival of both rod and cone cells. Thus, this system could find applications in understanding the basic photoreceptor physiology as well as in high throughput drug screening against all kinds of age related retinal blindness.

ACKNOWLEDGMENTS

This work was partly supported by DRDO CARS grant on the role of cerium oxide nanoparticles as a putative high altitude medicine (DIPAS/BSBE/20110112) and ISRO GOI grant on developing biomedical technologies to counter the deleterious effects of microgravity on the rod and cone photoreceptor network of the retina (STC/BSBE/20110064). M.D., K.B., and N.S. acknowledge the funding obtained from DIP-254 on cerium nanoparticles. This work is part of N.B.’s doctoral thesis.

¹S. Shahinfar, D. P. Edward, and M. Q. A. Tso, *Curr. Eye Res.* **10**, 47 (1991).

²S. Beatty, H. Koh, M. Phil, D. Henson, and M. Boulton, *Surv. Ophthalmol.* **45**, 115 (2000).

³D. Bok, *Proc. Natl. Acad. Sci.* **99**, 14619 (2002).

⁴F. Q. Liang and B. F. Godley, *Exp. Eye Res.* **76**, 397 (2003).

⁵S. G. Jarrett and M. E. Boulton, *Mol. Aspects Med.* **33**, 399 (2012).

⁶Y. Kuse, K. Ogawa, K. Tsuruma, M. Shimazawa, and H. Hara, *Sci. Rep.* **4**, 5223 (2014).

⁷P. R. MacLeish, C. J. Barnstable, and E. Townes-Anderson, *Proc. Natl. Acad. Sci. U. S. A.* **80**, 7014 (1983).

⁸J. W. Mandell, P. R. MacLeish, and E. Townes-Anderson, *J. Neurosci.* **13**, 3533 (1993).

⁹C. Gaudin, V. Forster, J. Sahel, H. Dreyfus, and D. Hicks, *Invest. Ophthalmol. Vis. Sci.* **37**, 2258 (1996).

¹⁰E. Balse, L. H. Tessier, C. Fuchs, V. Forster, J. A. Sahel, and S. Picaud, *Invest. Ophthalmol. Vis. Sci.* **46**, 367 (2005).

¹¹S. Skaper, “Isolation and culture of rat cone photoreceptor cells,” in *Neurotrophic Factors*, edited by S. D. Skaper (Humana, Totowa, NJ, 2012), pp. 147–158.

¹²N. Bhargava, V. Shanmugaiah, K. Balakrishnan, J. Ramkumar, and M. Das, *J. Biomater. Tissue Eng.* **5**, 431 (2015).

¹³D. Armstrong, G. Santangelo, and E. Connole, *Curr. Eye Res.* **1**, 225 (1981).

¹⁴M. Yamada, H. Shichi, T. Yuasa, Y. Tanouchi, and Y. Mimura, *J. Free Radical Biol. Med.* **2**, 111 (1986).

¹⁵M. O. Tso, *Trans. Am. Ophthalmol. Soc.* **85**, 498 (1987).

¹⁶L. R. Atalla, A. Sevanian, and N. A. Rao, *Curr. Eye Res.* **7**, 931 (1988).

¹⁷M. I. Naash and R. E. Anderson, *Exp. Eye Res.* **48**, 309 (1989).

¹⁸N. A. Rao, *Trans. Am. Ophthalmol. Soc.* **88**, 797 (1990).

¹⁹H. Yamashita, K. Horie, T. Yamamoto, T. Nagano, and T. Hirano, *Retina* **12**, 59 (1992).

²⁰M. A. De La Paz and R. E. Anderson, *Invest. Ophthalmol. Vis. Sci.* **33**, 2091 (1992).

²¹L. A. Bynoe, J. D. Gottsch, S. Pou, and G. M. Rosen, *Photochem. Photobiol.* **56**, 353 (1992).

²²S. G. Jarrett, H. Lin, B. F. Godley, and M. E. Boulton, *Prog. Retinal Eye Res.* **27**, 596 (2008).

²³K. Kunchithapautham and B. Rohrer, *Autophagy* **3**, 433 (2007).

²⁴H. Kokotas, M. Grigoriadou, and M. B. Petersen, *Clin. Chem. Lab Med.* **49**, 601 (2011).

²⁵S. J. Patel, F. Bany-Mohammed, L. McNally, G. B. Valencia, D. R. Lazzaro, J. V. Aranda, and K. D. Beharry, *Invest. Ophthalmol. Visual Sci.* **56**, 1665 (2015).

²⁶M. Das, S. Patil, N. Bhargava, J. F. Kang, L. M. Riedel, S. Seal, and J. J. Hickman, *Biomaterials* **28**, 1918 (2007).

²⁷M. Das, “Tissue engineering the motoneuron to muscle segment of the stretch reflex arc circuit utilizing micro-fabrication, interface design and defined medium formulation,” Doctoral thesis (Burnett School of Biomedical Sciences, University of Central Florida, 2008).

²⁸N. Bhargava, M. Das, A. Karakoti, S. Patil, K. J. Fong, S. Maria, K. Mark, S. Sudipta, and H. James, *J. Nanoneurosci.* **1**, 130 (2009).

²⁹K. Varghese, M. Das, N. Bhargava, M. Stancescu, P. Molnar, M. S. Kindy, and J. J. Hickman, *J. Neurosci. Methods* **177**, 51 (2009).

³⁰B. C. Nelson, M. E. Johnson, M. L. Walker, K. R. Riley, and C. M. Sims, *Antioxidants* **5**, 15 (2016).

³¹Y. Xue, Q. F. Luan, D. Yang, X. Yao, and K. B. Zhou, *J. Phys. Chem. C* **115**, 4433 (2011).

³²D. Schubert, R. Dargusch, J. Raitano, and S. W. Chan, *Biochem. Biophys. Res. Commun.* **342**, 86 (2006).

³³J. Chen, S. Patil, S. Seal, and J. F. McGinnis, *Nat. Nanotechnol.* **1**, 142 (2006).

³⁴C. Korsvik, S. Patil, S. Seal, and W. T. Self, *Chem. Commun.* 1056 (2007).

³⁵E. G. Heckert, A. S. Karakoti, S. Seal, and W. T. Self, *Biomaterials* **29**, 2705 (2008).

³⁶L. Kong, X. Cai, X. Zhou, L. L. Wong, A. S. Karakoti, S. Seal, and J. F. McGinnis, *Neurobiol. Dis.* **42**, 514 (2011).

³⁷M. Guo, J. Lu, Y. Wu, Y. Wang, and M. Luo, *Langmuir* **27**, 3872 (2011).

³⁸L. L. Wong, S. M. Hirst, Q. N. Pye, C. M. Reilly, S. Seal, and J. F. McGinnis, *PLoS One* **8**, e58431 (2013).

³⁹G. Ciofani, G. G. Genchi, B. Mazzolai, and V. Mattoli, *Biochim. Biophys. Acta* **1840**, 495 (2014).

⁴⁰S. K. Ujjain *et al.*, *Biointerphases* **9**, 31011 (2014).

⁴¹A. Arya, N. K. Sethy, M. Das, S. K. Singh, A. Das, S. K. Ujjain, R. K. Sharma, M. Sharma, and K. Bhargava, *Free Radical Res.* **48**, 784 (2014).

⁴²L. L. Wong, Q. N. Pye, L. Chen, S. Seal, and J. F. McGinnis, *PLoS One* **30**, e0121977 (2015).

⁴³L. Fiorani, M. Passacantando, S. Santucci, S. Di Marco, S. Bisti, and R. Maccarone, *PLoS One* **10**, e140387 (2015).

⁴⁴A. Arya, A. Gangwar, S. K. Singh, M. Roy, M. Das, N. K. Sethy, and K. Bhargava, *Int. J. Nanomed.* **2016**, 1159 (2016).

⁴⁵Q. Zhang, S. Fu, H. Li, and Y. Liu, *BioResources* **8**, 3699 (2013).

⁴⁶S. Taugaard, *Surface Analysis by Auger and X-ray Photoelectron Spectroscopy*, edited by D. Briggs and J. T. Grant (IM/Surface Spectra Ltd., Chichester, 2003), p. 295.

⁴⁷D. Briggs and M. P. Seah, *Practical Surface Analysis: Auger and X-ray Photoelectron Spectroscopy* (Wiley, Chichester, England, 1990).

⁴⁸E. E. Guibert, A. Y. Petrenko, C. L. Balaban, A. Y. Somov, J. V. Rodriguez, and B. J. Fuller, *Transfus. Med. Hemother.* **38**, 125 (2011).